

Raman scattering of acoustical modes of silicon nanoparticles embedded in silica matrix[†]

M. Ivanda,^{1*} A. Hohl,² M. Montagna,³ G. Mariotto,³ M. Ferrari,⁴ Z. Crnjak Orel,⁵ A. Turković¹ and K. Furić¹

¹ Ruđer Bošković Institute, 10002 Zagreb, Croatia

² Institute for Materials Science, Darmstadt University of Technology, Petersenstraße 23, D-64287 Darmstadt, Germany

³ Dipartimento di Fisica, Università di Trento and INFN, I-38050 Povo, Trento, Italy

⁴ Istituto di Fotonica e Nanotecnologie, CSMFO group, Via Sommarive 14, Trento, I-38050 Trento, Italy

⁵ National Institute of Chemistry, Hajdrihova 19, SI-1001 Ljubljana, Slovenia

Received 29 April 2005; Accepted 6 July 2005

The Raman scattering from acoustical phonons of silicon quantum dots in glass matrix was investigated. Two peaks that correspond to symmetric and quadrupolar spheroidal vibrations were found. A model calculation for in- and off-resonance scattering conditions was used, which considered the homogeneous broadening due to interaction with matrix and the inhomogeneous broadening due to particle size distribution. A strong dependence of the light-to-vibration coupling coefficient on the particles size was needed for fitting the Raman data. This result suggests that resonance with electronic transitions of the silicon nanoparticles is important for excitation at 514.5 nm. The size distribution obtained from the Raman data is in agreement with the results of high-resolution transmission electron microscopy. Copyright © 2006 John Wiley & Sons, Ltd.

KEYWORDS: silicon nanoparticles; spherical vibrational modes; size distribution; coupling coefficient

INTRODUCTION

Since the observation of strong photoluminescence (PL) in the visible region¹ emitted by nanosized porous Si, extensive experimental and theoretical studies have been done on the optical and structural properties of nanocrystallised silicon (nc-Si). PL spectra have been reported so far for a wide variety of nanostructures including porous Si and Si nanoparticles.^{2–4} Owing to the complexity of the PL properties, the origin of the PL in the visible region is not yet well understood. The prospect of realizing light-emitting devices stimulated intensive research of various nanometre-sized, Si-based structures using different types of preparative methods.⁵ One of the key issues in these studies is to clarify the quantum-size effects caused by the confinement of electrons and holes in zero-dimensional quantum dots. These properties are rather complex, being strongly dependent on the morphology, size, size distribution and nature of silicon nanoparticles.

Raman spectroscopy has been recognized as a powerful technique for the characterization of nanostructures. Particles of nanometre size show low-wavenumber vibrational modes that can be observed by Raman spectroscopy. These modes involve the collective motion of large numbers of atoms, and it is possible to calculate their wavenumbers using elasticity theory. It has been shown that the mean size and the width of the size distribution can be obtained from the shape of the Raman peaks.⁶ The purpose of this work is to extend similar studies to the case of silicon nanocrystals prepared by thermal decomposition of SiO amorphous structure by applying a model calculation that also considers the interaction of the crystalline particles with the surrounding glass. The size distribution obtained from the fit of the Raman spectra is compared to that measured by high-resolution transmission electron microscopy (HRTEM).

EXPERIMENTAL

The samples were prepared by Merck KGaA (Darmstadt, Germany) in an induction vacuum-sintering system by heating a Si/SiO₂ mixture to 1400 °C and subsequent condensation at 600 °C. The deposition rate was roughly 2 nm/s at a residual gas pressure of 10⁻⁶ bar and temperature of 300 °C. The samples were prepared on thin chromium-coated (of

[†]Presented as part of a commemorative issue for Wolfgang Kiefer on the occasion of his 65th birthday.

*Correspondence to: M. Ivanda, Ruđer Bošković Institute, P.O. Box 180, 10002 Zagreb, Croatia. E-mail: ivanda@irb.hr

a few hundred nanometre thickness) silicon substrates and silica substrates. Here we present the results on thermally annealed samples at 950 and 1100 °C on chromium-coated silicon substrates (S1 and S2 samples) and the sample annealed at 1100 °C on a silica substrate (S3 sample). Upon annealing in high vacuum, SiO decomposes into SiO₂ and elemental Si. After the decomposition, the excess Si atoms form Si clusters embedded in a SiO₂ matrix. The size of Si clusters is expected to become larger for higher annealing temperatures.

The Raman spectra were recorded by the DILOR Z-24 triple monochromator. An argon-ion laser (Coherent) with excitation line at 514.5 nm was used to record the spectra. The spectra were obtained in VV and VH polarization geometry (the excitation light vertically polarized and the scattering light vertically/horizontally analysed, with respect to the scattering plane). The spectra of the substrate were recorded separately and subtracted from the spectra with thin nc-Si/SiO₂ films. For the samples S1 and S2 the TO phonon line at 520 cm⁻¹ was used for the normalisation. For the sample S3, the strong, broad band with maximum at 440 cm⁻¹ was used for normalisation. To avoid heating by the laser, a cylindrical lens was used in focusing the excitation beam. Moreover, for the samples S1 and S2, the eventual heating was removed by the high-thermal-conducting chromium layer. All spectra were reduced (divided) with the Bose–Einstein factor ($n(\omega, T) + 1$), by using $T = 350$ K. HRTEM images were taken with a 200 kV microscope.

RESULTS AND DISCUSSION

The vibrations of elastic spheres have been studied a long time ago by Lamb⁷ and Love.⁸ The spherical case is well understood; the normal modes of the sphere can be divided into torsional and spheroidal ones. Tamura *et al.*⁹ extended the theoretical work by considering different surroundings and thus various boundary conditions for the spheroidal particles. Raman scattering from confined acoustic phonons has already been reported for some metal and semiconductor nanocrystals (NCs)^{10–13} and proteins.¹⁴ Furthermore, this technique was recently used to determine the crystallite size and size distributions in the nanometre range in insulators and semiconductors.^{15–17} The studied systems consist of NCs embedded in a glassy matrix,^{6,18} free-standing powders^{19–22} or colloidal solutions.^{23,24}

Low-wavenumber Raman experiments on nc-Si in SiO₂ also reveal broad peaks whose Raman positions scale inversely with the nanoparticle size.^{12,25–29}

The spheroidal and torsional modes are classified according to the symmetry group of the sphere by labels (l, m) as for the Harmonic functions Y_{lm} . Only the spheroidal modes of $l = 0$ and $l = 2$ are Raman-active.³⁰ The wavenumbers of the surface modes, i.e. the lowest energy mode of the $l = 0$,

2 sequences, for a free sphere are given by:

$$\nu_l = \frac{S_l v_l}{cD} \quad (1)$$

where ν_0, ν_2 are the wavenumbers of the surface symmetric and quadrupolar modes, D is the diameter of the spherical particle and c is the velocity of light. S_0 and S_2 are constants of the order of unity and depend on the ratio of the longitudinal and transverse sound velocities, $\nu_0 = v_L$ and $\nu_2 = v_T$ being the longitudinal and transverse sound velocities. The value of these coefficients as a function of v_L/v_T can be found in Ref. 31. Using the mean sound velocities of $v_L = 8790$ m/s and $v_T = 5410$ m/s for crystalline silicon, the values $S_0 = 0.76$ and $S_2 = 0.84$ are obtained. The quadrupolar mode is depolarized and appears in both the VV and VH polarization spectra at frequencies lower than the symmetric one, which appears only in VV polarization.

Figure 1 shows the polarized and depolarized Raman spectra of the S1–S3 samples. Both types of modes, symmetric and quadrupolar, are present in the spectra. The intense peak, present only in VV spectra is attributed to the $l = 0$ surface mode and the weaker one at lower wavenumber, to the quadrupolar $l = 2$ mode. The wavenumber ratios of these peaks, 1.56, 1.44, and 1.46 for the S1, S2, and S3 samples, respectively, agree well with the calculated value $\nu_0/\nu_2 = 1.53$, strongly suggesting the assignment of these peaks to $l = 0$ and $l = 2$ modes.

The width of the peaks has an inhomogeneous contribution related to the size distribution and a homogeneous contribution due to the interaction of the particle with the surrounding glass.

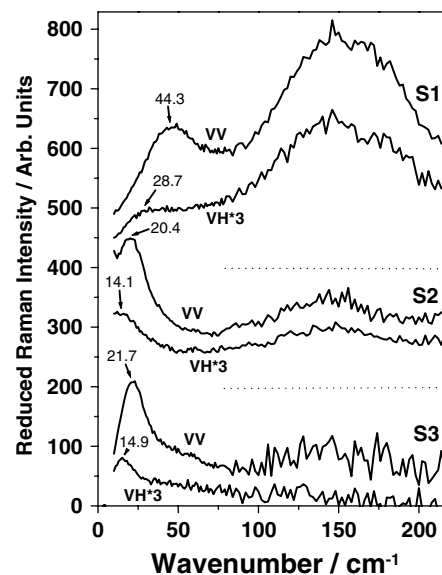


Figure 1. Low-wavenumber VV and VH polarized Raman spectra, reduced for the Bose–Einstein factor, of different nc-Si in SiO₂. The higher-reported peak wavenumber corresponds to the symmetric mode, $l = 0$, and the lower one to the quadrupolar mode, $l = 2$.

The Raman spectrum of spatially confined vibrations is generally described by the Shuker and Gammon relation³²

$$I_l(\nu, T) = \frac{n(\nu, T) + 1}{\nu} C_l(\nu)g(\nu) \quad (2)$$

where $C_l(\nu)$ is the light-to-vibration coupling coefficient, $g(\nu)$ is the density of vibrational states, T is the temperature, and $n(\nu, T) + 1$ is the Bose–Einstein occupation factor for the Stokes component.

For off-resonance conditions, it has been shown that the light-to-vibration coupling coefficient is proportional to the particle diameter,³¹ $C(D) \approx D$. The density of vibrational states, $g(\nu)$, corresponds to the size distribution $N(D)$, since each particle vibrates with frequencies that are inversely proportional to the diameter D . It seems that the distribution of small particles is well approximated with a log-normal size distribution:^{13–16}

$$N(D) \propto \exp \left[-\frac{(\ln(D/D_0))^2}{2\sigma^2} \right] \quad (3)$$

Here, D_0 is the diameter that corresponds to the maximum of the distribution and the parameter σ measures the distribution width.

For nanoparticles interacting with an elastic surrounding matrix, the vibrational modes are further damped because of the interaction with matrix, and $C_l(\nu)$ is no more a sharp function of the frequency. This effect is known as a homogeneous line broadening. The homogeneous line shape $C_l(\nu)$ can be calculated if the densities, the longitudinal and transverse sound velocities of the nanoparticle and matrix are known.³¹ In this case, the Raman scattering intensity, reduced for trivial Bose–Einstein temperature population factor, i.e. $I^R(\nu) = I(\nu)/(n(\nu) + 1)$, for an ensemble of nanoparticles with size distribution $N(D)$ is given by the integral of the homogeneously broadened Raman spectrum over the inhomogeneous distribution:

$$I_l^R(\nu) = \frac{I_l(\nu)}{n(\nu) + 1} = \int \frac{C_l(\nu, D)}{\nu} N(D) dD \quad (4)$$

Figure 2(a) shows $C(\nu)/\nu$ calculated for the symmetric mode of a free silicon particle and that of a silicon particle in a silica glass matrix. The calculation was performed by the method of Montagna and Dusi.³¹ The effects of inhomogeneous broadening for the non-resonant case (when $C \approx D^1$) calculated by Eqn (4) is also shown on the same figure. Figure 2 (b)) shows the calculated effects of inhomogeneous broadening for the case with $C \approx D^7$, which gives the best fit with the experimental data, and it will be discussed later. The wavenumber downshift and line broadening as a function of the distribution width is shown in Fig. 3. It is evident that the wavenumber downshift for the same distribution width is much larger for the $C \approx D^7$ case.

In order to fit the observed spectra with the calculated ones, first we subtract the contribution of quadrupolar mode

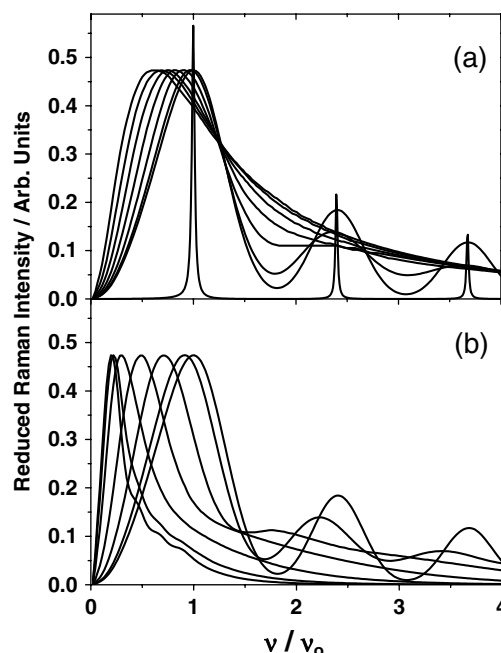


Figure 2. (a) Reduced Raman spectra of the symmetric mode of nc-Si, calculated for a free nanoparticle (spectrum with the sharp lines); for a nanoparticle in the glass matrix, the homogeneously broadened spectrum and inhomogeneously broadened by log-normal size distributions with different σ parameters (broad peaks). The first broadened spectrum is for $\sigma = 0$ (only homogeneous broadening) and the other broader spectra are calculated by increasing the parameter σ in steps of 0.1. The wavenumbers are normalized to the value of the symmetric mode ν_0 of the free nanoparticle. (b) the same as in (a) but for resonant-scattering conditions $C(D) \approx D^7$.

in VV Raman spectra. The depolarization ratio for the $l = 2$ mode is a system-dependent quantity. It should be in the range between 1/3, the value for cubic systems and dipole-induced dipole mechanism of scattering (in the off-resonant case),³¹ and 3/4, the value for randomly oriented molecules. We used the value 1/3, but the result is not very critically dependent on the choice, since the intensity of the $l = 2$ peak in VV spectra is smaller than that of the $l = 0$ peak. After subtraction, the resulting spectrum, $I_{VV} - 3 \times I_{VH}$ should contain the symmetric mode only. Figure 4 shows such difference Raman spectra for the three samples. Besides the symmetric mode in the spectra, there is an additional peak at $\sim 150 \text{ cm}^{-1}$, which corresponds to the transverse acoustical-(TA-) phonon-like band that appears in amorphous and crystalline silicon whenever strong phonon confinement is present. This peak is more polarized than the quadrupolar one and, therefore, is still present in the difference spectra. The spectra were fitted with Eqn (4) by using log-normal distribution $N(D)$ and the peak intensity, σ and D_0 as fitting parameters. The TA band was fitted with a Gaussian peak with a fixed width of 40 cm^{-1} for all the spectra. The fit was

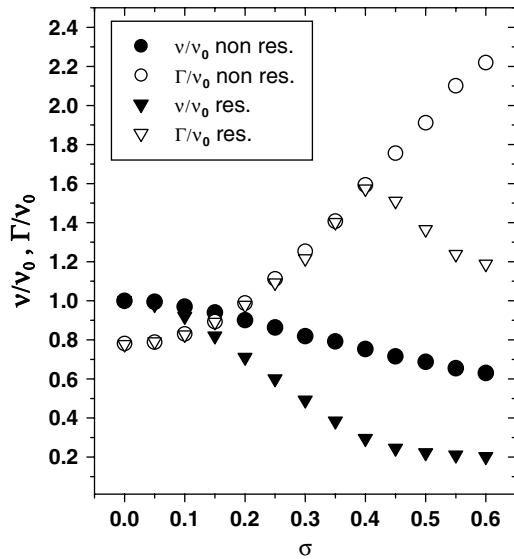


Figure 3. Wavenumber ν and the full width at half-maximum, Γ , of the symmetric mode of nc-Si in a glass matrix inhomogeneously broadened with different size distributions as a function of the parameter of the distribution width, σ . The values are normalized to the wavenumber of the free Si nanoparticle.

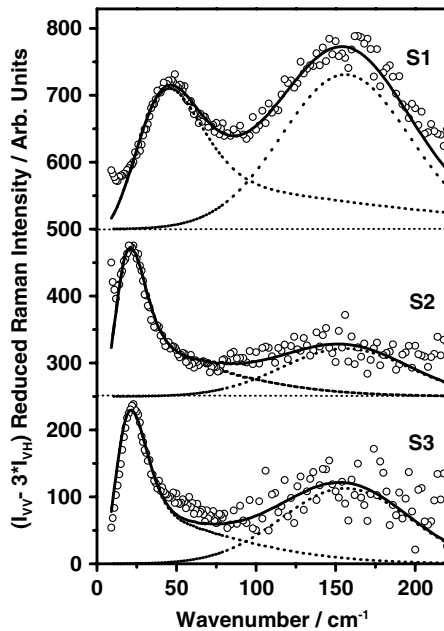


Figure 4. $I_{VV} - 3 \times I_{VH}$ reduced Raman spectra fitted with the TA peak at $\sim 150 \text{ cm}^{-1}$ (width of 38 cm^{-1}) and nc-Si symmetric mode (dashed lines) inhomogeneously broadened because of particles size distributions in resonant-scattering conditions. The sum of both contributions is given by the continuous line. The parameters D_0 and σ are results of the fit.

performed by using a power law expression, $C(D) \approx D^\alpha$, for the coupling coefficient and taking α as a free parameter.

The non-resonant case ($\alpha = 1$) was also calculated. The best simultaneous fit on the Raman and HRTEM data was obtained with $\alpha = 7$.

The size distributions found from the fit are shown in Fig. 5 and compared with the corresponding HRTEM distributions. The size distributions in the two cases are in excellent agreement, but only by assuming a coupling coefficient strongly dependent on the particle size, $C(D) \approx D^7$. The fit for the non-resonant case ($C(D) \approx D$) gives a significantly larger particle size. Our results are in agreement with those of Fujii *et al.*¹² in that case also, the sizes estimated from the wavenumbers of the acoustic modes of Si crystallites were much larger than those observed by TEM. Similar observation was also made by Pauthe *et al.*²⁶ Fujii *et al.*¹² ascribed this phenomenon to the large anisotropy of the elastic constants and to the matrix effects. On the basis of the present results, one can rule out that the disagreement is due to a matrix effect, which was considered in the calculation. In fact, the interaction with the matrix broadens and shifts the lines towards lower wavenumbers, but this shift is much smaller than that expected. We can also exclude the possibility that the effects are due to the anisotropy of the elastic constants: in the detailed study of molecular dynamics of large clusters of silicon, Saviot *et al.*²⁷ found a relatively good agreement between the calculated wavenumbers of the anisotropic Si sphere and those of the Lamb sphere with isotropic sound velocities, the average values for different direction of propagation. A third possibility for such an observation could be the presence of a layer around the crystalline silicon particles, possibly of amorphous silicon, not visible by TEM, but belonging to the particle from the point of view of the vibrational dynamics. However, it is

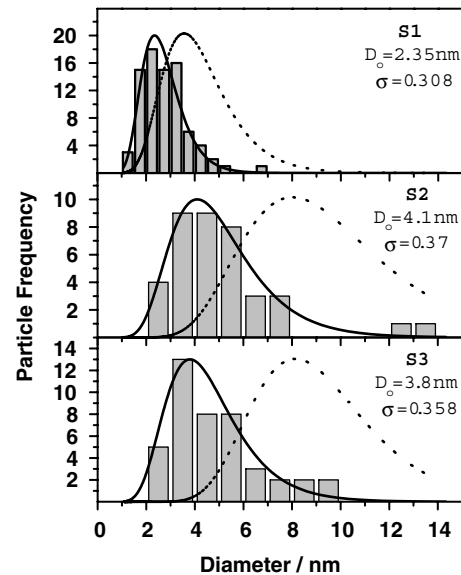


Figure 5. Comparison of HRTEM size distributions and those obtained from the Raman spectra in resonant (bold line) and non-resonant (dashed line) scattering conditions.

difficult to explain why the volume ratio of the amorphous and crystalline parts of the particles should increase with the mean particle size, as observed in the present case.

As discussed earlier, a good agreement between Raman and HRTEM data is obtained by assuming a strong size-dependence of the Raman coupling coefficient, as that described by $C(D) \approx D^7$. The physical mechanism for such an effect could be a resonance with the excitonic transitions, which should be strongly size-dependent. The condition of resonant Raman excitation are proved by the measurements of absorption on Si nanocrystallites, where strong resonant (band gap) absorption at an energy of 2.41 eV has been observed³³ for the particles larger than 2.1 nm. Therefore, for all samples analysed here, almost all silicon particles are resonantly excited. To explain the strong dependence of the coupling coefficient on the particle diameter, i.e. $C \approx D^7$, the role of the electronic levels needs to be taken into account. The problem has been recently studied for the case of metallic particles, where resonance with the surface plasmon excitation has been shown to be the physical mechanism of intense low-wavenumber Raman scattering from acoustic vibrations.³⁴

The recent Raman scattering results on acoustic modes in silicon nanoparticles doped with erbium²⁹ are quite different from those of the present work and of other previous studies.^{12,26} It seems that when erbium atoms are placed on the surface of nc-Si, the observed wavenumber of the symmetrical mode is in agreement with Eqn (1), and that there is no need for invoking resonance effects. However, it seems unlikely that the presence of Er can change the mechanism of inelastic light scattering, and the origin of the observed difference is not clear. Off-resonance measurements, by exciting in the red, could probably clarify the problem. Unfortunately, the intensity of the Raman scattering for red excitation is very weak, further indicating that resonance effects are important, and these measurements have not been yet reported.

CONCLUSIONS

In conclusion, the acoustical modes in the Raman spectra of different nanocrystalline samples in SiO₂ matrix have been analysed. Symmetric and quadrupolar spheroidal modes were found. A model calculation that included interaction with matrix and size distribution was performed. The observed Raman spectra were explained with a resonant-scattering model, where a strong dependence of the light-to-vibration coupling coefficient on the size of silicon nanoparticle was found to exist. In this way, a good agreement between the size distribution obtained from the Raman data and HRTEM measurements was obtained.

REFERENCES

1. Canham LT. *Appl. Phys. Lett.* 1990; **57**: 1046.

2. Takagi H, Ogawa H, Yamazaki Y, Ishizaki A, Nakagiri T. *Appl. Phys. Lett.* 1990; **56**: 2379.
3. Morisaki H, Ping FW, Ono H, Yazawa K. *J. Appl. Phys.* 1991; **70**: 1869.
4. Littau KA, Szajowski PJ, Muller AJ, Kortan AR, Brus LE. *J. Phys. Chem.* 1993; **97**: 1224.
5. Ossicini S, Pavesi L, Priolo F. *Light Emitting Silicon for Microphotonics, Springer Tracts in Modern Physics* Vol. 194. Springer-Verlag: Berlin, 2003.
6. Ivanda M, Babocsi K, Dem C, Schmitt M, Montagna M, Kiefer W. *Phys. Rev., B* 2003; **67**: 235329.
7. Lamb H. *Proc. Math. Soc. Lond.* 1882; **13**: 187.
8. Love AEH. *A Treatise on Mathematical Theory of Elasticity*. Dover: New York, 1944.
9. Tamura A, Higeta K, Ichinokawa T. *J. Phys. C: Solid State Phys.* 1982; **15**: 4975.
10. Haro-Poniatowski E, Jouanne M, Morhange JF, Kanehisa M, Serna R, Afonso CN. *Phys. Rev., B* 1999; **60**: 10080.
11. Mariotto G, Montagna M, Viliiani G, Duval E, Lefra S, Rzepka E, Mai C. *Europhys. Lett.* 1988; **6**: 239.
12. Fujii M, Nagareda T, Hayashi S, Yamamoto K. *Phys. Rev., B* 1996; **54**: R8373.
13. Champagnon B, Adrianasolo B, Ramos A, Gandais M, Allais M, Benoit JP. *J. Appl. Phys.* 1993; **73**: 2775.
14. Painter PC, Mosher LE. *Biopolymers* 1982; **18**: 3121.
15. Champagnon B, Andrianasolo B, Duval E. *Mater. Sci. Eng. B* 1991; **9**: 417.
16. Duval E, Boukenter A, Champagnon B. *Phys. Rev. Lett.* 1986; **56**: 2052.
17. Jouanne M, Morhange JF, Kanehisa M, Haro-Poniatowski E, Fuentes GA, Torres E, Tellez Hernandez E. *Phys. Rev., B* 2001; **64**: 155404.
18. Montagna M, Moser E, Visintainer F, Zampedri L, Ferrari M, Martucci A, Guglielmi M, Ivanda M. *J. Sol.-Gel Sci. Technol.* 2003; **26**: 241.
19. Ivanda M, Tonejc AM, Djedj I, Gotić M, Musić S, Mariotto G, Montagna M. *Lecture Notes in Physics: Nanoscale Spectroscopy and Its Applications to Semiconductor Research*, Watanabe Y, Heun S, Salviati G, Yamamoto N (eds). Springer Verlag: Heidelberg 2002; 16.
20. Ivanda M, Musić S, Gotić M, Turković A, Tonejc AM, Gamulin O. *J. Mol. Struct.* 1999; **480–481**: 641.
21. Ristic M, Ivanda M, Popovic S, Musić S. *J. Non-Cryst. Solids* 2002; **303**: 270.
22. Gotić M, Ivanda M, Sekulic A, Music S, Popovic S, Turkovic A, Furic K. *Mater. Lett.* 1996; **28**: 225.
23. Verma P, Cordts W, Irmer G, Monecke J. *Phys. Rev., B* 1999; **60**: 5778.
24. Genzel L, Keilmann F, Martin TP, Winterling G, Yacoby Y, Fröhlich H, Makinen MW. *Biopolymers* 1976; **15**: 219.
25. Liu FQ, Liao L, Wang G, Cheng G, Bao X. *Phys. Rev. Lett.* 1996; **76**: 604.
26. Pauthe M, Bernstein E, Dumas J, Saviot L, Pradel A, Ribes M. *J. Mater. Chem.* 1999; **9**: 187.
27. Saviot L, Murray DB, del C. Marco de Lucas M. *Phys. Rev., B* 2004; **69**: 113402.
28. Murray DB, Saviot L. *Phys. Rev., B* 2004; **69**: 094305.
29. Wu XL, Mei YF, Siu GG, Wong KL, Moulding K, Stokes MJ, Fu CL, Bao XM. *Phys. Rev. Lett.* 2001; **86**: 3000.
30. Duval E. *Phys. Rev., B* 1992; **46**: 5795.
31. Montagna M, Dusi R. *Phys. Rev., B* 1995; **52**: 10 080.
32. Shuker R, Gammon RW. *Phys. Rev. Lett.* 1970; **25**: 222.
33. Furukawa S, Miyasato T. *Phys. Rev., B* 1988; **38**: 5726.
34. Bachelier G, Mlayah A. *Phys. Rev., B* 2004; **69**: 205408.